Numerical Simulation of The Influence of Geometric Parameter on The Flow Behavior in a Solar Chimney Power Plant system

Prof. Dr. Arkan khilkhal Husain Mechanical Engineering Dep. University of Technology Email: alaalwn@yahoo.com

Asst.Prof.Dr Waheeds Shate Mohammad Mechanical Engineering Dep University of Technology Email: alaalwn@yahoo.com

Lecturer. Abbas JassimJubear Mechanical Engineering Dep. University of Wassit Email:Abbaskut72@yahoo.com.au

ABSTRACT

Numerical simulations have been carried out on the solar chimney power plant systems. This paper gives the flow field analysis for a solar chimney power generation project located in Baghdad. The continuity, Naver-stockes, energy and radiation transfer equations have been solved and carried out by Fluent software. The governing equations are solved for incompressible, 3-D, steady state, turbulent is approximated by a standard $\mathbf{k-\varepsilon}$ model with Boussiuesq approximation to study and evaluate the performance of solar chimney power plant in Baghdad city of Iraq. The different geometric parameters of project are assumed such as collector diameter and chimney height at different working conditions of solar radiation intensity (300,450,600,750 and 900 W/m^2) to gain the optimal designed structure. The results show that the change of collector diameter and chimney height has considerable effects on the performance of the system. The velocity increase when the collector diameter and chimney height increase and reach to the maximize value at H=D 12 m and when solar intensity (900 W/m^2). The study shows that Iraqi weather are suitable for this system.

Keywords: Solar chimney; Solar energy; Collector; Natural convection.

نمذجة رقمية لتاثير المعاملات الهندسية على سلوك الجريان في منظومة مدخنة شمسية لتوليد القدرة

أ. د.اركان خلخال حسين قسم هندسة الميكانيك/الجامعة التكنولوجية

أ.م.د. وحيد شاتي محمد قسم هندسة الميكانيك/الجامعة التكنولوجية

م. عباس جاسم جبير قسم هندسة الميكانيك/جامعة واسط

الخلاصة

تم اجراء محاكات عددية على نظام محطة المدخنة الشمسية للطاقة.تبين هذه الدراسة تحليل لحقل الجريان لمشروع محطة المدخنة الشمسية للطاقة في بغداد. تم حل معادلات الاستمرارية,Naveries-Stokes, الطاقة والاشعاع الشمسي باستخدام برنامج Fluent(14).في هذه الدراسة تم حساب اداء المدخنة الشمسية من خلال حل المعادلات الحاكمة خلال جريان لانظغاطي ,ثلاثي الابعاد,مستقر واضطرابي حيث تم الاستعانة بالموديل الاضطرابي (k-ε) في اجواء بغداد-العراق.خلال هذه الدراسة تم فرض عدد من المتغيرات الهندسية المختلفة مثل قطر المجمع الشمسي و ارتفاع المدخنة الشمسية وذلك عند ضروف اختبار مختلفة من شدة الاشعاع الشمسي (300,450,600,750,900) واط/م^2 وذلك لغرض التوصل الى افضل تصميم. من ابرز النتائج التي تم التوصل اليها , ان قطر المجمع وارتفاع المدخنة له تاثير كبير على متغيرات اداء النظام. تزداد السرعة داخل المدخنة الشمسية بزيادة قطر المجمع وارتفاع المدخنة وتصل الى اقصى قيمه لها عندما كان قطر المجمع وارتفع المدخنة (12 م) وعند شدة اشعاع شمسي (900 واط/م^2). ان اجواء العراق تعتبر ملائمة لهذا النوع من الانظمة.

الكلمات الرئيسيه: مدخنه شمسيه, الطاقه الشمسيه, مجمع, الحمل الحر

1. INTRODUCTION

A solar chimney power plant, SCPP is a solar thermal power plant that uses greenhouse principle (solar air collector) and buoyancy effect created by a chimney to generate a solar induced convective flow which drives pressure staged turbogenerator(s) to generate electricity, A traditional solar chimney power plant consists of a circular transparent canopy or roof raised a certain height above the ground, with a chimney/tower at its center as shown in **Fig. 1**. The chimney at the center houses one or more turbogenerator(s) located at its base. Ambient air from the surrounding enters the system along the circumference of the collector roof and the ground. Radiation from the sun penetrates the collector roof and strikes the ground surface and the heated ground in turns heats the adjacent air from the ambient temperature to warm air temperature at the collector outlet. The Warm air underneath the collector moves toward and up into the central chimney as a result of buoyancy and pressure difference between the ambient air and the warm air inside the plant. The kinetic energy in the warm air is converted to electrical energy using turbogenerator (s), **Aja, and Hussain, 2011.** Detailed theoretical preliminary research and a wide range of wind tunnel experiments led to the establishment of an experimental plant with a peak output of 50 kW on a site made in Manzanares (about 150 km south of Madrid) in 1981/82. The experimental plant in Manzanares operated for about 15,000 hours from 1982 onwards. In Australia a 200MW solar tower project is currently being developed**, Schlaich, et al., 2005,Bergermann, and Partenr, 2002, and www.wikipedia.org. Maia et al, 2009,** presented a theoretical analysis of a turbulent flow inside a solar chimney. They showed that the most important physical elements in a solar chimney system are the tower dimensions as they cause the most significant variation in the flow behavior. An increase in the height and diameter of the tower produces the rise in the mass flow rate and decrement in the flow temperature. **Bernardes et al. 2009.** developed a validated mathematical model to estimate the temperature and power output of solar chimneys. The maximum power can be reached when the factor pressure drop at the turbine is equal to approximately 0.97 from the total potential pressure. The other parameters were also involved in the study such as; distance between absorber and ground, double cover area, water-storage system area and thickness. The results showed that their effect was insignificant since the energy output was the same. Similarly, **Backström et al., 2006**. found that maximum fluid power was available at a much lower flow rate and much higher turbine pressure drop than the constant pressure potential assumption given. **Koonsrisuk & Chitsomboon, 2009.** studied the ventilation efficiency of solar chimney by comparing between five of the mathematical simulations and five of CFD simulations both from the previous researches. Moreover, **Maia et al., 2009.** presented a validated numerical simulation showed that the height and diameter of the tower were the most significant physical variables for solar chimney design. The maximum chimney height for convection avoiding negative buoyancy at the latter chimney and the optimal chimney height for maximum power output were presented and analyzed by, **Zhou et al., 2009.** using a theoretical model validated with the measurements of the prototype in Manzanares. The results showed that maximum height gradually increased with the lapse rate increasing and go to infinity at a value of around 0.0098 K/ m. **Walter, and Sergio,1984.** described the design, construction and testing the variation in the geometry of the chimney for solar dryer system, the results indicated that a slight geometry modification of the chimney (convert cone keeping height constant) will increase air velocity by a factor of 2- 3 with respect to a chimney of cylindrical shape. **Bernardes et al., 2003.** developed a model to estimate the power output of solar chimneys and to examine the effect of various ambient conditions and structural dimensions of the power output. **Zhou et al., 2007.** built a pilot experimental solar chimney thermal power generating equipment in China. They carried out a simulation study to investigate the power generating system performance

based on a developed mathematical model. **Ming Tingzhen et al., 2006.** advanced a model to evaluate the performance of a solar chimney power plant system, in which the effects of various parameters(chimney and collector) on the relative static pressure, driving force, power output and efficiency have been further investigated. **Tingzhena et al., 2008.** presented a numerical simulation of the solar chimney power plant systems coupled with turbine. **Mathur et al., 2006.** presented experimental investigations on solar chimney for room ventilation and **Bassiouny, and Koura, 2008.** presented an analytical and numerical study of solar chimney used for room natural ventilation.

In the present study we modeled a 3-D solar chimney power plant which includes the parts of the ground, collector, and chimney together. The flow details production of plants with different dimensions and different solar intensities are presented.

2. NUMERICAL IMPLEMENTATIONS

Advanced solver technology provides fast, accurate CFD results, flexible moving and deforming meshes, and superior parallel scalability. Computational Fluid Dynamics (CFD) procedures solve all the interacting governing equations in a coupled manner, albeit in a finite framework. With a careful use of CFD, its results could be used to validate those of the theoretical models, at least qualitatively.

2-1 Modelling in GAMBIT

For the simulation part, the model is designed by using GAMBIT 2.4.6 for this configuration. This software is provided with the advanced geometry and meshing tools. The functions of GAMBIT are design the three dimensional (3-D), setup the boundary condition for each edge and faces ,and provide the meshing analysis for each configuration.

The solar chimney power plant was modeled with the following dimensions, Circular absorber ground with the different diameter of (6,8,10 and 12 m), inclined collector angle (θ = 0°), different chimney height (6,8,10 and 12 m), chimney diameter 0.3 m and the gap between the absorber and the transparent cover (glass) is 0.1m as shown in **Fig.2**.

The numerical examination of the flow behavior of air under the steady state condition was studied at both the inlet and the chimney base where the turbine is expected to be staged. The fluid flow calculation was simulated using FLUENT software. The buoyancy driven flow in the system was assumed to be turbulent based on previous studies. Set up the boundary condition is to define the situation occur at the surface condition in term of friction. Meanwhile, defining the meshing is vital in order to discrete each part to certain section for more accuracy FLUENT's analysis. It is important to define model, meshing, and boundary conditions before running into FLUENT.

Proper boundary conditions are needed for a successful computational work. After creating a geometry which have one volume defined the specify boundary types of solar collector, solar chimney and the base such as the wall , while the entry and exit zones type is Inlet and Outlet-Pressure. Now The assembly is meshed using tetrahedral elements of T-grid scheme type, **Jinhua, et al., 2007.** Gambit scheme with spacing interval size (0.0275) is chosen as shown in **Fig. 3**, the Gambit grid generator with approximately (2-4.5) million computational cells for different cases. No-slip condition for velocity and temperature on the walls.

2-2 Simulation with FLUENT

FLUENT solves the governing integral equations for the conservation of mass, momentum, energy, and other scalers, such as turbulence.There are two processors used to solve the flow and heat transfer equations. The first preprocessor is the program structure which

creates the geometry and grid by using GAMBIT. The second post processor is solving Navier-Stokes equations which include continuity, momentum and energy.

The set of conservation equations used by CFD are:

Mass conversion equation

$$\frac{\partial \rho}{\partial t} + \frac{\partial}{\partial x_i}(\rho u_i) = 0 \quad (1)$$

Momentum.

In x-direction

$$\rho[U\frac{\partial U}{\partial x} + V\frac{\partial U}{\partial y} + W\frac{\partial U}{\partial z}] - \frac{\partial p}{\partial x} + \frac{\partial}{\partial x}[\mu\frac{\partial U}{\partial x} - \overline{\rho u' u'}][\frac{\partial}{\partial y}\left[\mu\frac{\partial U}{\partial y} - \overline{\rho u' v'}\right] + \frac{\partial}{\partial z}[\mu\frac{\partial U}{\partial z} - \overline{\rho u' w'}]S_U \quad (2)$$

In y-direction

$$\rho\left[U\frac{\partial V}{\partial x} + V\frac{\partial V}{\partial y} + W\frac{\partial V}{\partial z}\right] = -\frac{\partial p}{\partial y} + \frac{\partial}{\partial x}[\mu\frac{\partial V}{\partial x} - \overline{\rho u' v'}] + [\frac{\partial}{\partial y}[\mu\frac{\partial V}{\partial y} - \overline{\rho v' v'}] + \frac{\partial}{\partial z}[\mu\frac{\partial V}{\partial z} - \overline{\rho v' w'}] + S_V \quad (3)$$

In z-direction

$$\rho[U\frac{\partial W}{\partial x} + V\frac{\partial W}{\partial y} + W\frac{\partial W}{\partial z}] - \frac{\partial p}{\partial z} + \frac{\partial}{\partial x}[\mu\frac{\partial W}{\partial x} - \overline{\rho u' w'}] + [\frac{\partial}{\partial y}[\mu\frac{\partial W}{\partial y} - \overline{\rho v' w'}] + \frac{\partial}{\partial z}[\mu\frac{\partial W}{\partial z} - \overline{\rho w' w'}] + S_W \quad (4)$$

Energy.

$$\rho[U\frac{\partial T}{\partial x} + V\frac{\partial T}{\partial y} + W\frac{\partial T}{\partial z}] = \frac{\partial}{\partial x}[\frac{\mu}{\sigma_T}\frac{\partial T}{\partial x} - \overline{\rho u' t'}] + [\frac{\partial}{\partial y}[\frac{\mu}{\sigma_T}\frac{\partial V}{\partial y} - \overline{\rho v' t'}] + \frac{\partial}{\partial z}[\frac{\mu}{\sigma_T}\frac{\partial V}{\partial z} - \overline{\rho w' t w'}] \quad (5)$$

The viscous medium is also taken. the analysis is carried using turbulent flow and then the standard k-epsilon is considered and take standard wall functions near wall functions, **Launder, and Spalding, 1972.** The Boussinesq approximation is used to estimate the effect of density variation with temperature.Selecting a radiation model enables radiation heat transfer. Discrete Ordinates (DO) was selected under this model and then selected DO Irradiation under the solar load model .Define the solar parameters, Enter values for the X, Y, and Z components of the Sun Direction Vector.

In the current study used different direct solar irradiation (300 ,450 ,600 ,750 ,900 W/m^2) data were obtained from Ministry of Transportation-Iraqi Meteorological Organization And Seismology of Baghdad city of 8-8-2008 in the following times (7:30 , 8:15 , 9 ,10 A.M. and 12:30 P.M.) and the sun direction vector obtained from, **John, 1980.**

Boundary conditions specify the flow and thermal variables on the boundaries of the physical model. They are, therefore, a critical component of the FLUENT simulations and it is

important that they are specified appropriately. The boundary conditions applied in this research are those shown in **Table 1., Ming, et al., 2006.** Initially the first order upwind scheme was used to get a napproximate solution. This solution is then used as the initial conditions for the second order up wind solver.

3- SIMULATION RESULTS

In order to validate the results of the numerical part of the present work, a comparison with the numerical study of, **Rafah, 2007.** was carried out. It can be seen from **Fig. 4,** and **5** the absorbing ground temperature and exit velocity when using asphalt aggregates as an absorption background, with (0.1m) periphery of collector at radiation intensities of (310,415,505 W/m^2). A good agreement with the numerical results is achieved.

3-1 Variation of the Solar Intensity and Sunlight Direction

The results of the temperature distribution and velocity vectors of solar insolation (300,450,600,750,900 W/m^2) at times of (7:15,8:15,9,10 AM and 12:30 PM) with D=12m and H =10m regarding the solar chimney passage are presented in **Figs. 6. to 11.** The increase in air velocity is very small up to about half the radius of the collector. The very steep increase is obtained in the inner half of the collector. This trend is noticed in all solar intensities and sunlight direction as shown in **Figs. 6.** and **7** The reason is the combined effect of flow area reduction and the amount of the heat transfer from the ground to the working fluid, which increases the kinetic energy of the flow particles. To compare the velocities of the air at the solar collector passage for different solar intensity times (7:30,8:15,9,10 AM and 12:30 PM) generally, it could be seen that the maximum velocity occurs in the (900W/m^2) solar radiation intensity at (12:30 PM) and the minimum velocity in the morning with (300W/m^2) solar intensity at (7:15AM). The numerical solution has shown that the velocity in the center of the chimney is higher than near the wall. This is logical and in agreement with measurements of real fluid in rounded passages.

The variations in the air temperature through the collector passage, i.e. in the radial direction are found to be very gradually as shown in **Figs. 8.** and **9** for different solar insolations. The temperature near the ground is high compared with other regions. Consequently, the density near the walls is lower. Generally, along the collector passage, the temperature is increased but the density and pressure decreased. It is clear from the figures that the air enters the collector at ambient temperature and is heated as it moves toward the chimney. The temperature gradient present in the air is steeper near the collector inlet as the boundary layer is thinner in this zone than in regions closer to the chimney.

The development of flow in the chimney can be seen through the enlargement regions shown in **Figs. 10.** and **11**. The flow in the lower and middle regions is developing non uniform flow, but in the top region is uniform fully developed flow (turbulent flow). The velocity increases when the chimney height and collector diameter increase.

To compare the temperatures of air at the ground, collector diameter at different solar intensity and sunlight direction, it can be seen that the maximum temperature occurs in insolation of (900W/m^2) at (12:30 Am) because the solar radiation intensity is very high compared to other times, as shown in **Figs. 12.** and **13**. Figures also show a strong temperature drop at the collector center when the solar intensity is (600,750, and 900 W/m^2 because the velocity in this point is very low, which is a stagnation point.

The velocity profiles from ground to top chimney for different solar intensities, shown in **Figs. 14.** and **15**. The numerical results indicate that air velocity shows a large increase near surface of the ground about (0.3m to 0.4m) chimney height and then the increase of air velocity reduced, and the maximum velocity occur near the top of the chimney. Furthermore, the turbine may be positioned at a higher position when the velocity is large to improve power output.

3-2 Collector Diameter Variation

The maximum air temperature differences between inlet and absorbing ground occurred at the larger diameter due to the collector area exposed to the incident radiation with different solar intensities (300-900W/m^2), as in **Fig. 16.** The increase of the collector diameter means, the area of the absorbing ground is increased and the air temperature in the system is increased too, which result in the decrease in air density. Thereby, the static pressure in the system increased and the driving force increased accordingly. **Fig. 17**. shows the computed updraft velocities at the end section of the chimney for all test cases, as a function of solar intensity. All distributions display the expected increasing trend with the insolation. The rates of an increase of the velocities appear to be slightly lower as the insolation increases. Furthermore the increase in collector diameter causes an increase in temperature so the velocity will be increased too.

3-3 Chimney Height Variation

The simulations were carried out for chimney heights of (6m, 8m,10m, and 12m). The results show that an increase in the height of the chimney causes an increase in the pressure drop along the chimney, causing greater mass flow rates and higher flow velocity. As observed, larger mass flows and velocities cause a reduction in local temperature values as shown in **Figs. 18.** and **19**. It is clear from **Figs. 20.** and **21**, that as chimney height increased then buoyancy force will increase so one can anticipate increase the air velocity with increasing chimney height.

3-4 Temperature Distrbution at a Different Height Above the Ground

The distribution of air temperature at different heights above ground level are shown in **Figs. 22.** and **23.** The variations of air temperature within the collector near the ground (h=0m), at height (h=0. 05m) above the ground level, and at the inner glass collector surface (h=0. 1m). Air temperatures decrease with an increase in height above ground level, which is induced by the greenhouse effect. Solar radiation firstly heat the absorber bed, which heat the cool air nearly. Cool air obtains heat mainly by free convection and radiation. The temperature of the ground is higher in the region due to the storage heat in the bed, while the inner glass has a minimum temperature because the glass acts as a bed conducting material on hard and passes most of the radiation.

4- CONCLUTION

A theoretical analysis of the turbulent flow inside a solar chimney was presented. Flow was modeled through the numerical solution of the conservation equations of mass, energy, and momentum, as well as the turbulent variables transport equations. The model includes a flow detail inside a collector and chimney. Numerical simulations were conducted in order to evaluate the performance of solar chimney power plants with different dimensions. This observation would be useful in the preliminary plant design. The results show:

1. The numerical results and figure of this study have a good agreement with the numerical results of, Rafah, 2007. at the same conditions.
1. The maximum air temperature was 80.29C°, at (D=12m and H=6m).

2. Maximum outlet air velocity was 4.91 m/s, at (D=12m and H=12 m).
3. Both, maximum air temperature and exit air velocity were at solar radiation intensity; 900 W/m^2.
4. Almost, increasing in collector diameter leads to increased air temperature and velocity.
5. The increasing in chimney height leads to decreasing of air temperature but increasing in velocity.
6. Under the Iraqi weather radiation conditions, large scale solar chimney in Iraq is recommended for a power plant.

REFERENCES

Aja, O.C., and Hussain, H., 2011, *Review on the Enhancement Techniques and Introduction of an Alternate Enhancement Technique of Solar Chinmey Power Plant*, Journal of Applied Sciences, ISSN 1812-5654/DOI: 10,3929.

Backström, T. W., and Fluri, T. P.,2006, *Maximum fluid power condition in solar chimney power plants – an analytical approach*, Int. J Solar Energy, Vol.80, PP.1417-1423

Bassiouny R., and Koura NSA., 2008, *An analytical and numerical study of solar chimney use for room natural ventilation*, Energ Buildings Vol.40, PP.865–873.

Bergermann, S., and Partner, 2002, *The Solar Chimney", Structural Consulting Engineers*.

Bernardes, M. A., Dos, S., Backström, T. W., and Kröger, D. G.,2009, *Analysis of some available heat transfer coefficients applicable to solar chimney power plant collectors*. *Int. J Solar Energy*, Vol.83, PP. 264–275.

Bernardes MA dos S., and Weinrebe G., 2003, *Thermal and technical analyses of solar chimneys*. Sol Energy, Vol.75, PP.511–524.

Jianhua F., Louise J.and Simon F.,2007, *Flow Distribution in a Solar Collector Panel with Horizontally Inclined Absorber Strips*, http://www.sciencedirect.com, Solar Energy, Vol. 81, PP. (1501–1511),2007.

John A. D.,1980, *Solar Engineering of Thermal Processes*, Book, John Wiley and SONS , INC.,Second Edition.

Koonsrisuk, A., and Chitsomboon, T.,2009, *Accuracy of theoretical models in the prediction of solar chimney performance*, Solar Energy, Vol.38, PP. 1764-1771.

Launder, B. E. and Spalding, D. B.,1972, *Lectures in Mathematical Models of Turbulence*, Academic Press, London, England.

Maia, C. B., Ferreira, A. G., Valle, R. M., and Cortez, M. F. B., 2009, *Theoretical evaluation of the influence of geometric parameters and materials on the behavior of the airflow in a solar chimney*, *Computer & Fluid*, Vol.38, PP. 625–636.

Mathur J., Bansal NK., Mathur S., and Jain M., 2006, *Anupma. Experimental investigations on sol chimney for room ventilation*, Sol Energy, Vol.80, PP.927–935.

Ming Tingzhen, Liu Wein Y.Z. and Xu Guoliang, 2006, *Analytical and numerical investigation of the solar chimney power plant systems*, International Journal of Energy Research, Vol. 30, PP.861–873.
Ming T., Liu W., and Xu G., 2006, *Analytical and Numerical Investigation of the Solar Chimney Power Plant Systems*, International Journal of Energy Research, Vol. 30, Issue 11, PP. (861–873).

Rafah A. N., 2007, *Numerical Prediction of a Solar Chimney Performance Using CFD Technique*, Ph.D. Thesis Submitted to Electromechanical Engineering Department University of Technology Baghdad.

Schlaich, J., Bergermann, R., Schiel,W., and Weinrebe, G., 2005, *Design of Commercial Solar Updraft Tower Systems – Utilization of Solar Induced Convective Flows for Power Generation*.

Tingzhena M., Weia L., Guolinga X., Yanbina X., Xuhua G., and Yuanb P., 2008, *Numerical simulation of the solar chimney power plant systems coupled with turbine* , Renew Energy Vol.33, PP.897–905.

Walter Z., and Sergio A., 1984, *Design Construction and testing of a Chimney that Reduces Dangerous Temperature in a radiative Convective Solar Dryer*, Solar Energy, Vol. 32, NO.5.
4- www.wikipedia.org

Zhou X, Yang J, Xiao Bo, and Hou G. ,2007, *Simulation of a pilot solar chimney thermal power generating equipment*, Renew Energy, Vol.32, No.10, PP.1637–1644.

Zhou X., Yang, J., Xiao, B., Hou, G. and Xing, F.,2009. *Analysis of chimney height for solar chimney power plant*, Applied Thermal Engineering,Vol.29, PP.178–185.

SYMBOLS AND ACRONYMS

Symbol	Description	Unit
D	Diameter of absorbing ground	m
g	Gravitational acceleration	m/s^2
H	Chimney height	m
h	Heat transfer coefficient	W/m^2k
I	Solar radiation	W/m^2
K	Turbulent kinetic energy	m^2/s^2
p	Pressure	Pa
S_ϕ	General source term	
T	Temperature	C°

t	Time	s
u' , v'	Fluctuation of mean velocities	m/s
U,V, W	Time-average velocity	m/s
u, v,w	Velocity components (x,y&z) direction	m/s
Δ	Differentive	
α	Absorbtance	
∂	Partial derivative	
ε	Rate of dissipation of kinetic energy	m^2/s^2
θ	Angle	degree
ρ	Fluid density	kg/m3
μ	Dynamic viscosity	$N.s/m^2$
μ_t	Turbulent viscosity	N.s/m2
π	Pi	
o	Ambient	

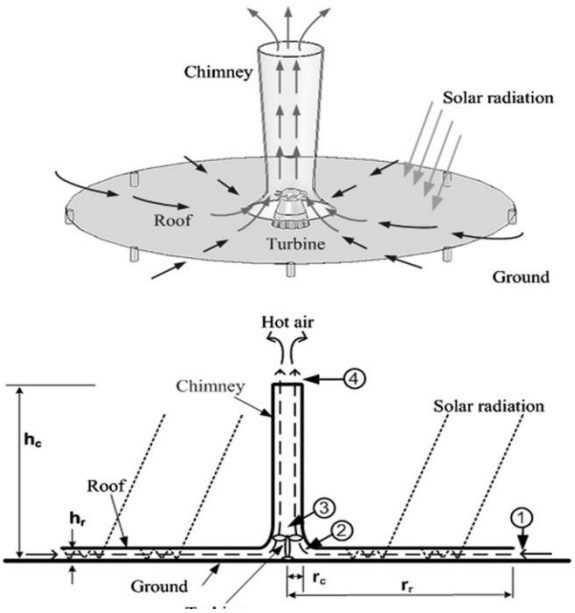

Figure 1. Schematic layout of the conventional solar chimney power plant.

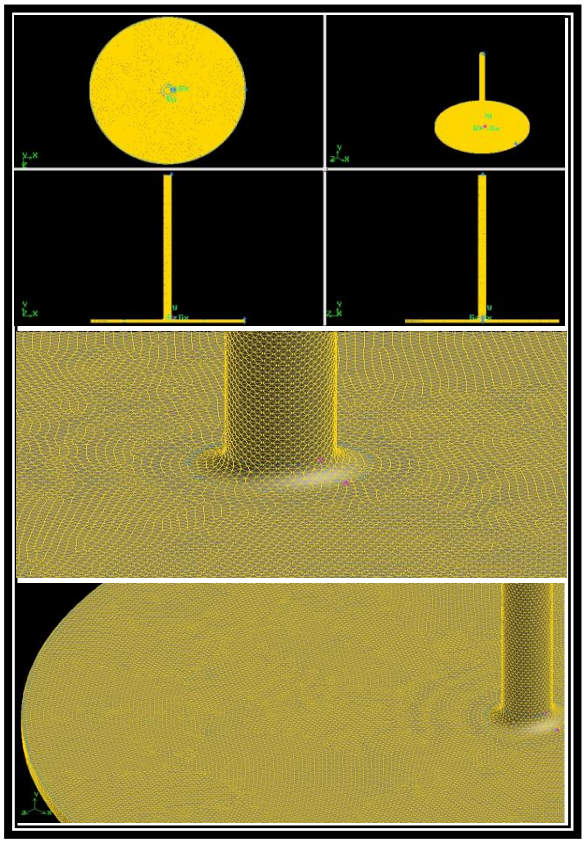

Figure 3. Computational grad.

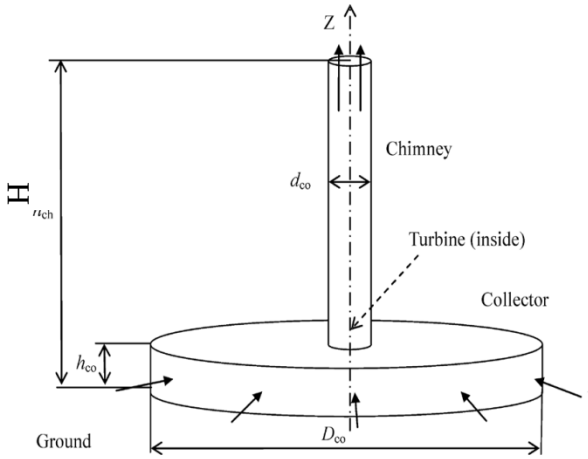

Figure 2. Physical prototype

Table 1. Boundary conditions in detail.

Boundary	**Type**	**Boundary condition**
Inlet	Pressure - inlet	ΔP=0 ; T= $T_{ambient}$;
Exit	Pressure -out let	ΔP=0; $T = T_{ambient} - 0.0065*$ *chimney height*
Ground (asphalt)	Wall	Thermal condition: Mixed h=8 W/m^2K;T=T_{ambint}
Chimney Wall	Wall	Constant heat flux: q=0
Glass(semi-transparent)	Wall	Thermal condition: Radiation(Thicness= 0.004mm

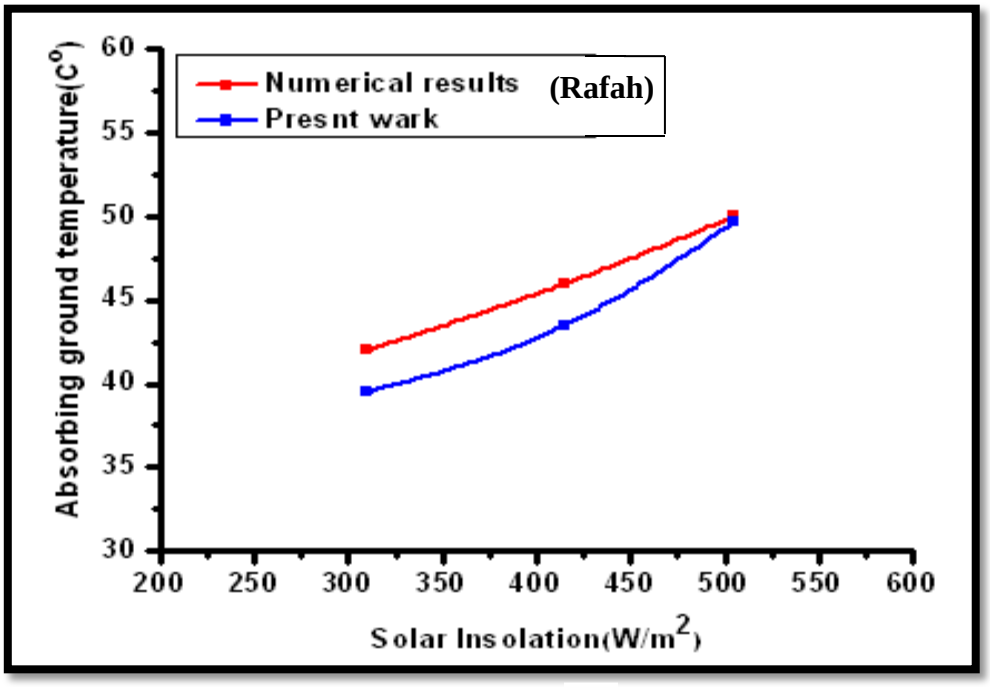

Figure 4. Variation in absorbing ground temperature with solar insolation comparing, with an numerical study.

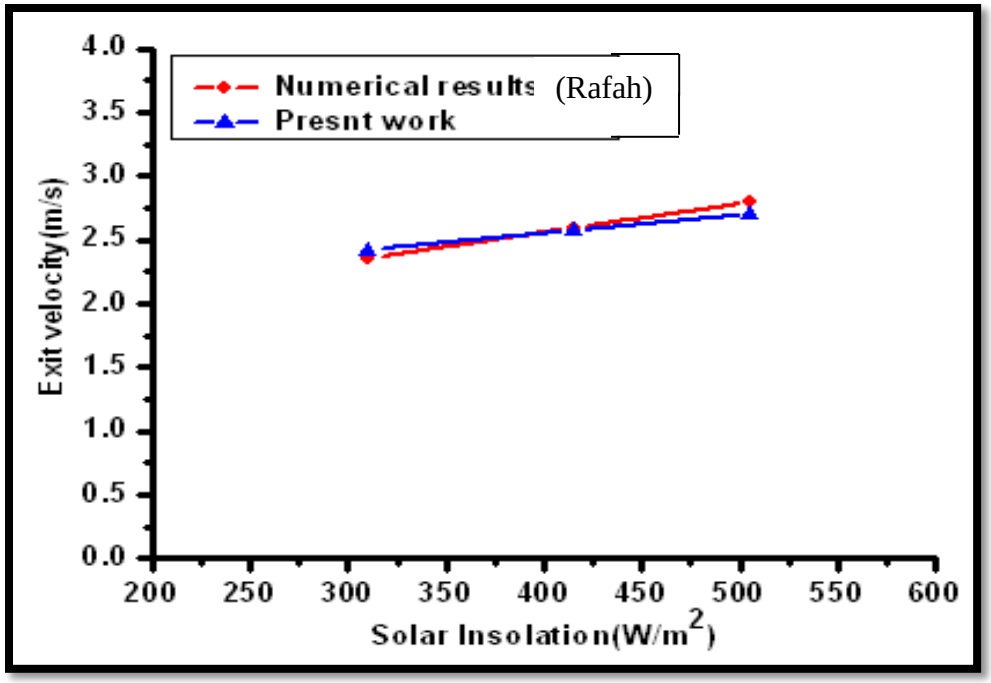

Figure 5. Variation in exit air velocity with solar insolation comparing, with an numerical study.

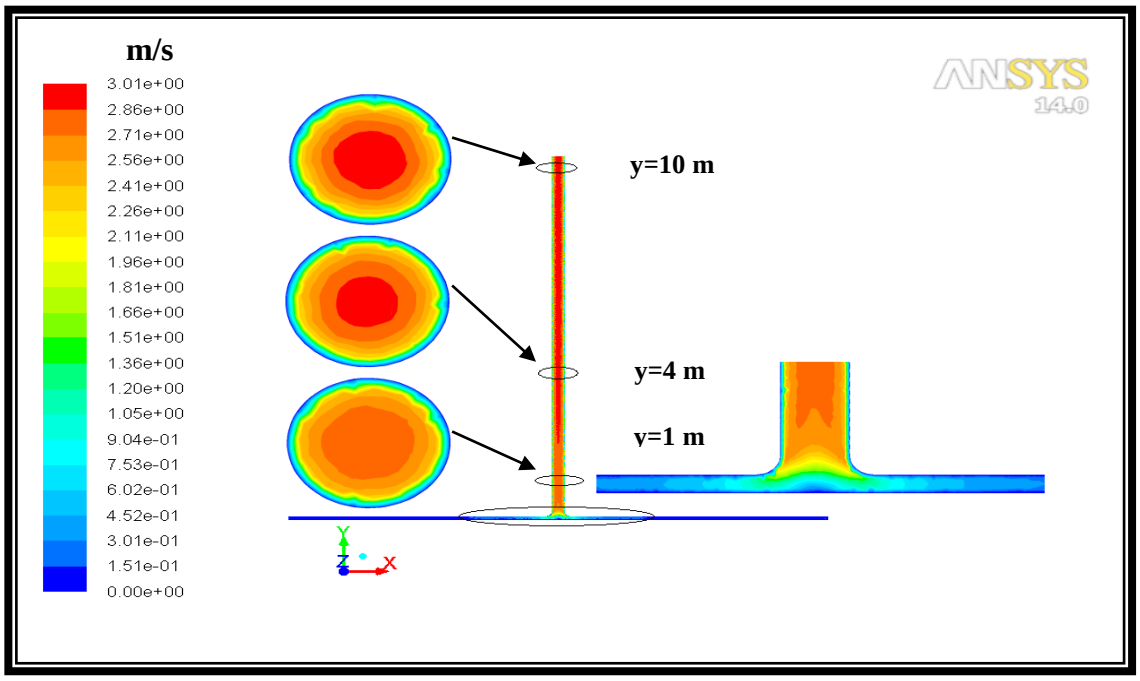

Figure 6. Velocity distribution contours of the solar chimney with solar insolation (300 W/m^2) for D=12m, H=10m.

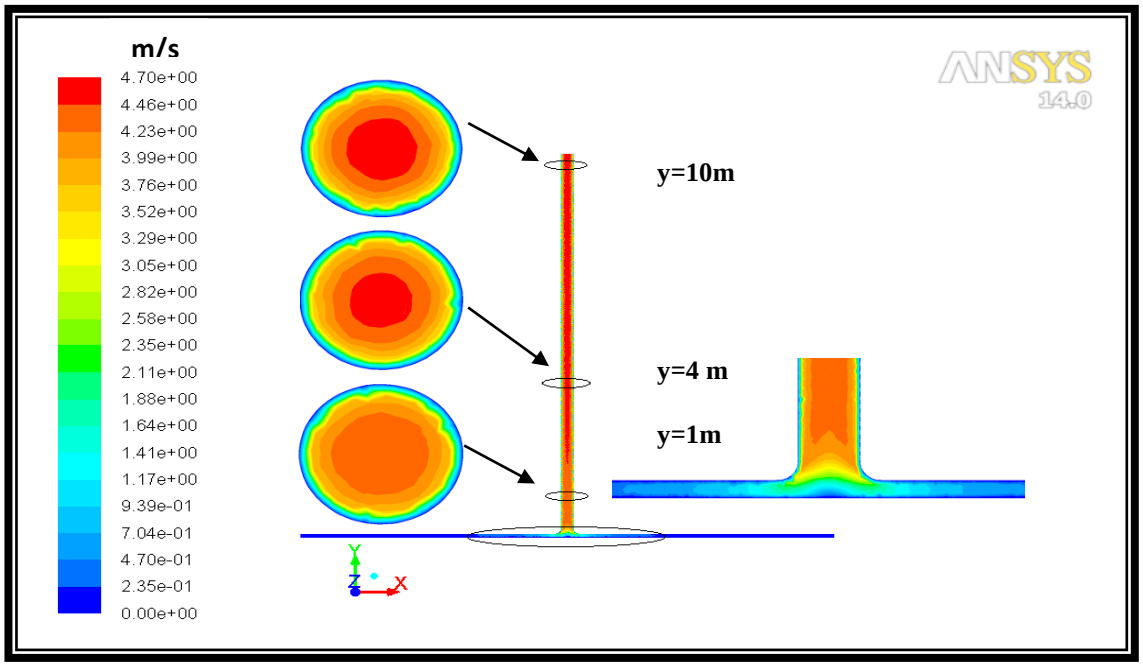

Figure 7. Velocity distribution contours of the solar chimney with solar insolation (900 W/m^2) for D=12m, H=10m.

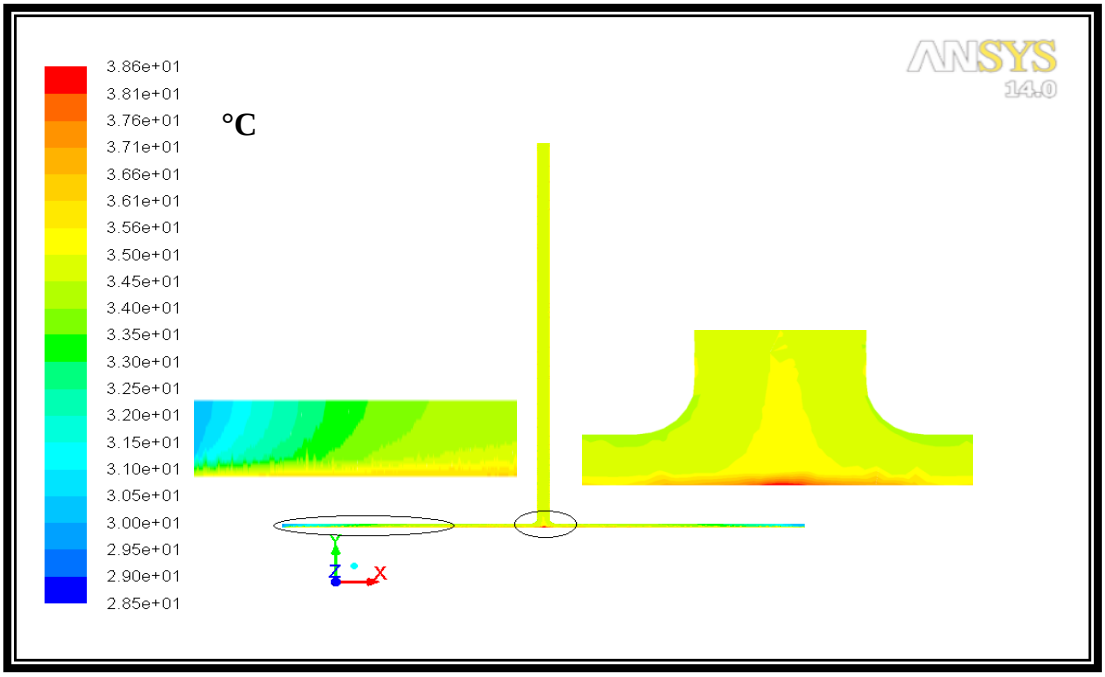

Figure 8. Temperature distribution contours of the solar chimney with solar insolation (300 W/m^2) for D=12m, H=10m.

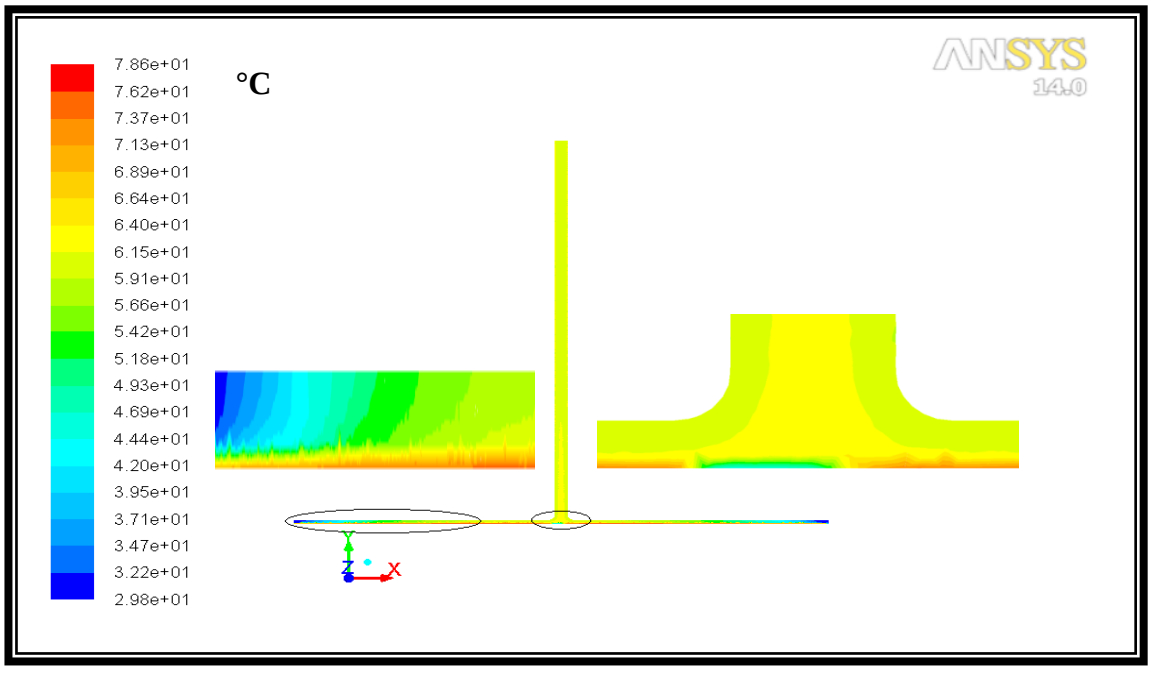

Figure 9. Temperature distribution contours of the solar chimney with solar insolation (900 W/m^2) for D=12m, H=10m.

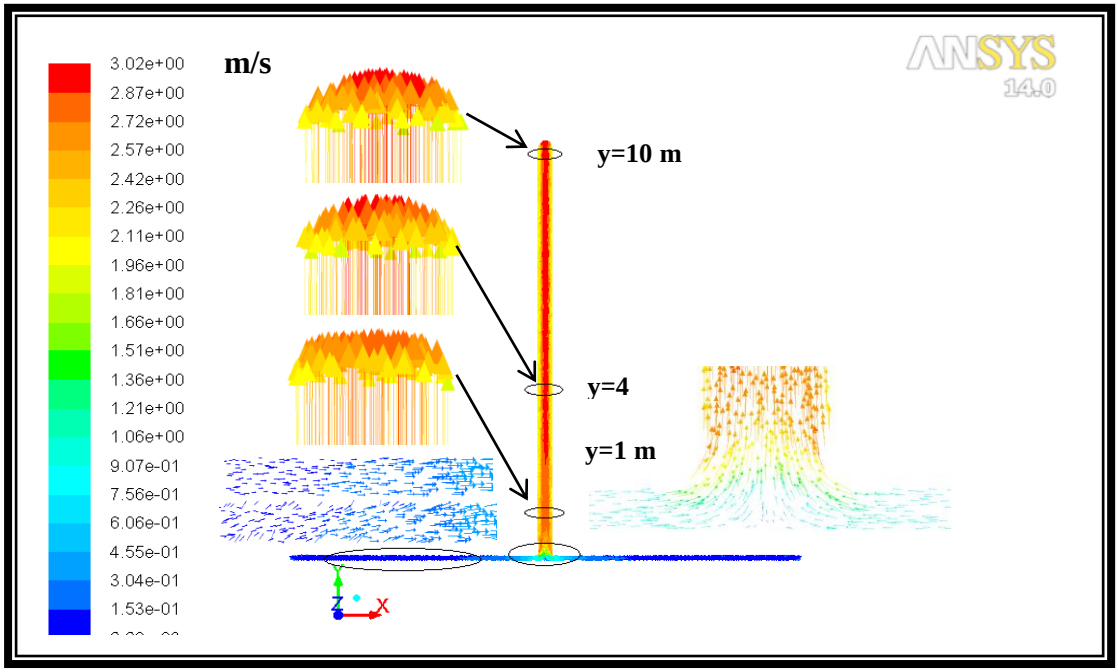

Figure 10. Flow felid of air in solar chimney with solar insolation (300 W/m^2) for D=12m, H=10m.

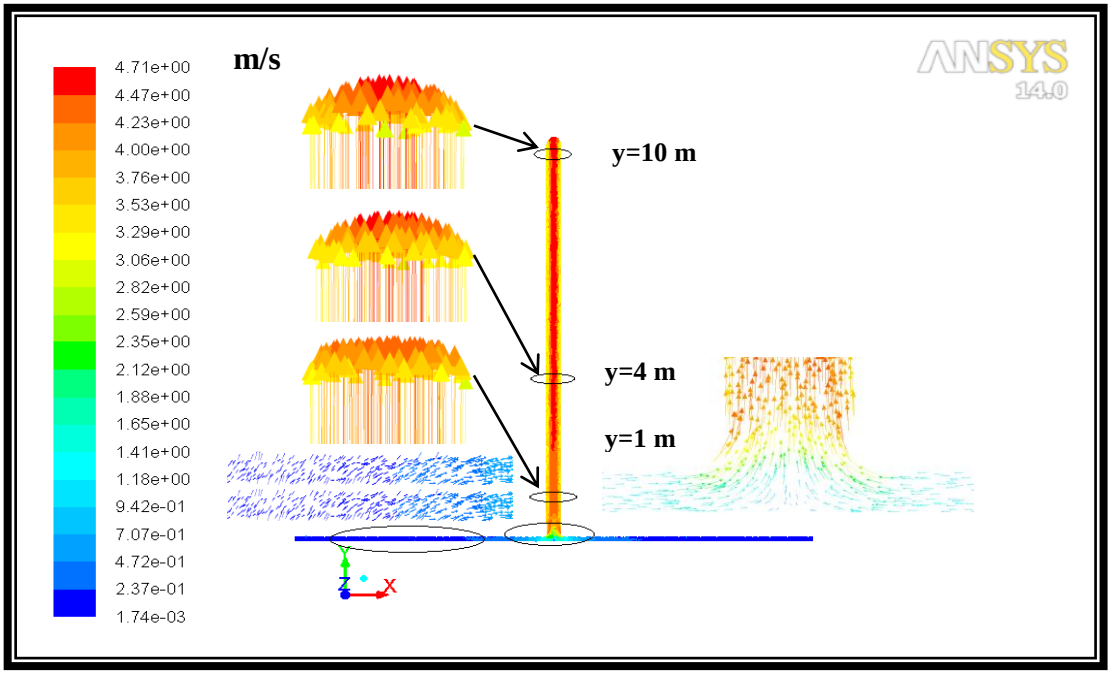

Figure 11. Flow felid of air in solar chimney with solar insolation (900 W/m^2) for D=12m, H=10m.

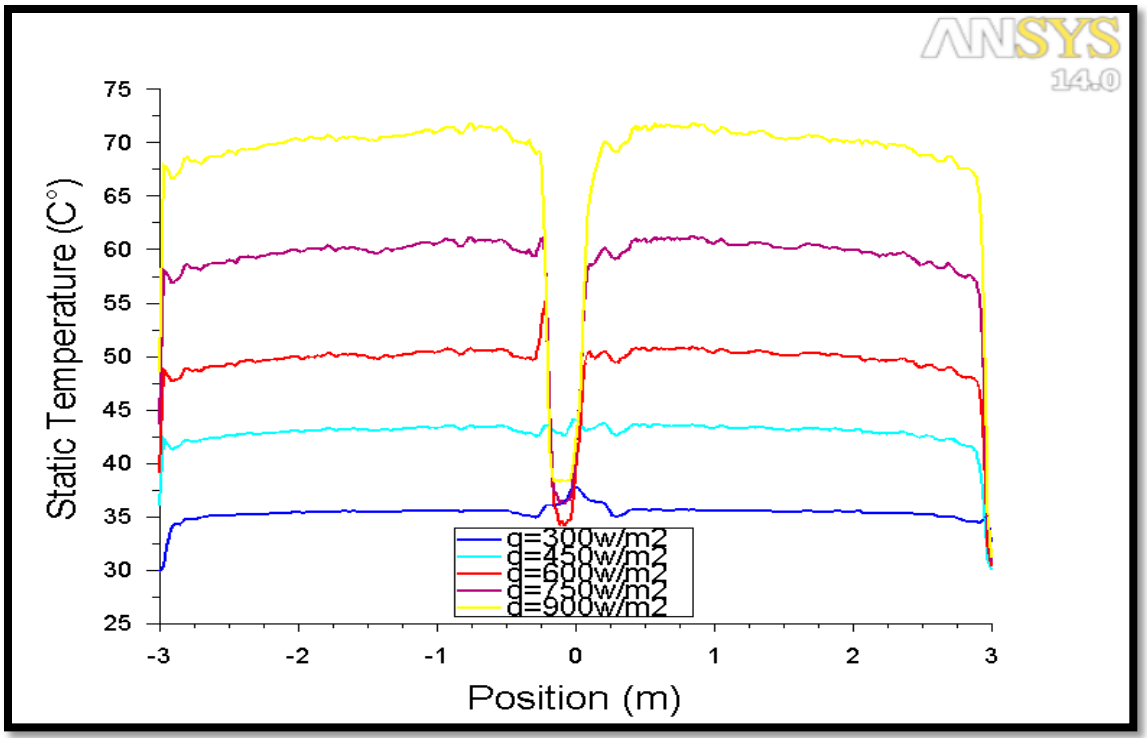

Figure 12. Ground temperature variation from solar collector diameter at different solar insolation for D =6m, H =6m.

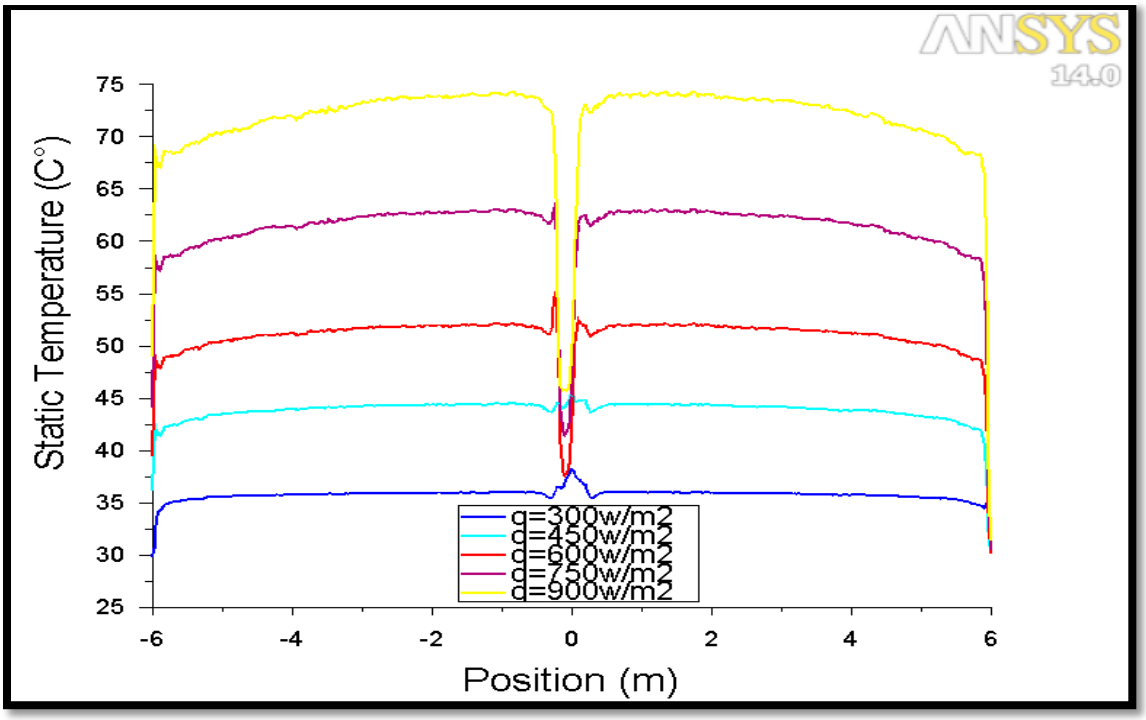

Figure 13. Ground temperature variation from solar collector diameter at different solar insolation for D =12m, H =12m.

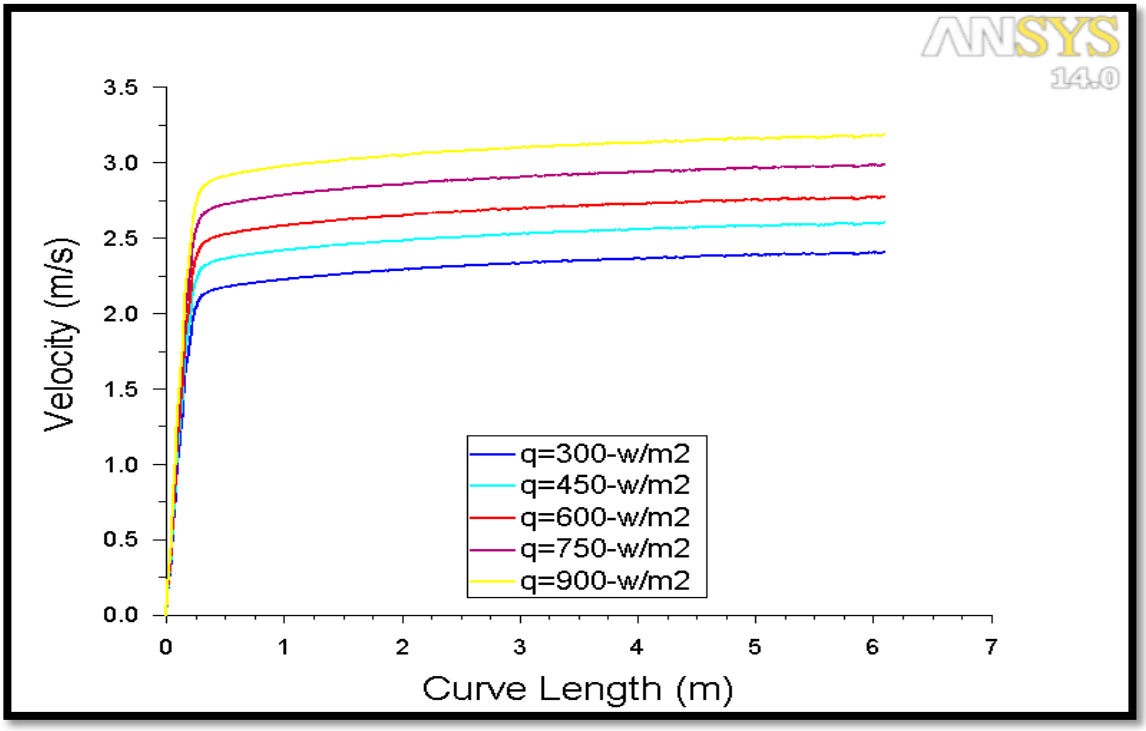

Figure 14. Air velocity variation from center collector exit to chimney exit at different solar insolation for D =6m, H =6m.

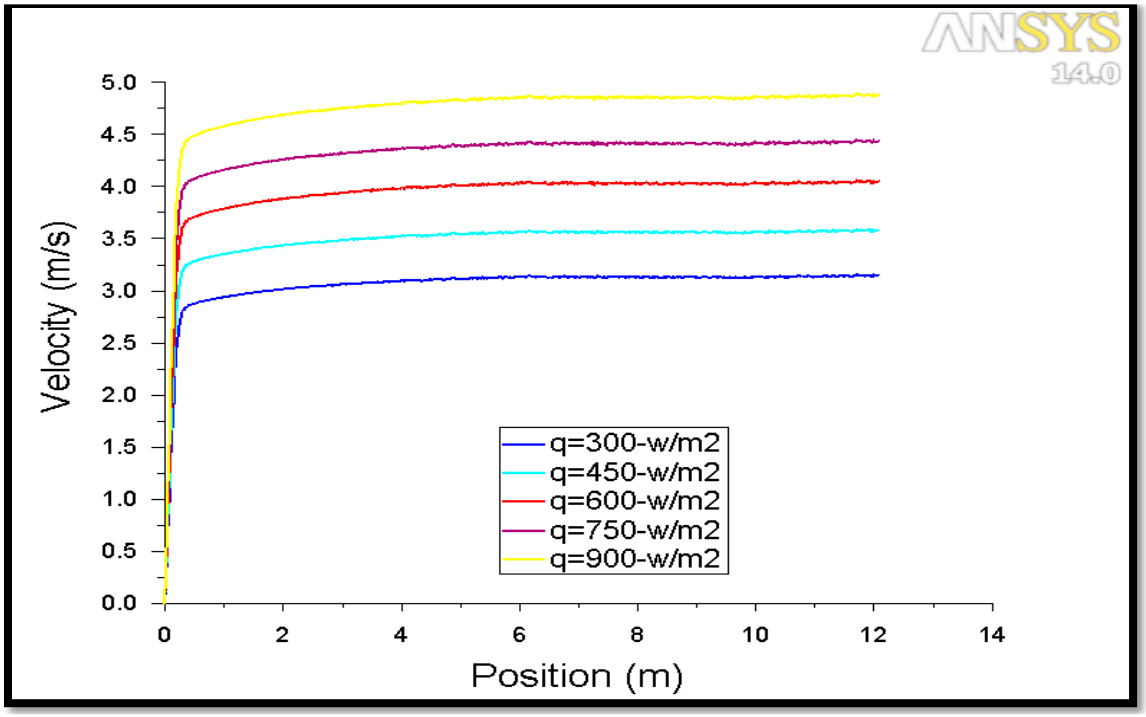

Figure 15. Air velocity variation from center collector exit to chimney exit at different solar insolation for D =12m, H =12m.

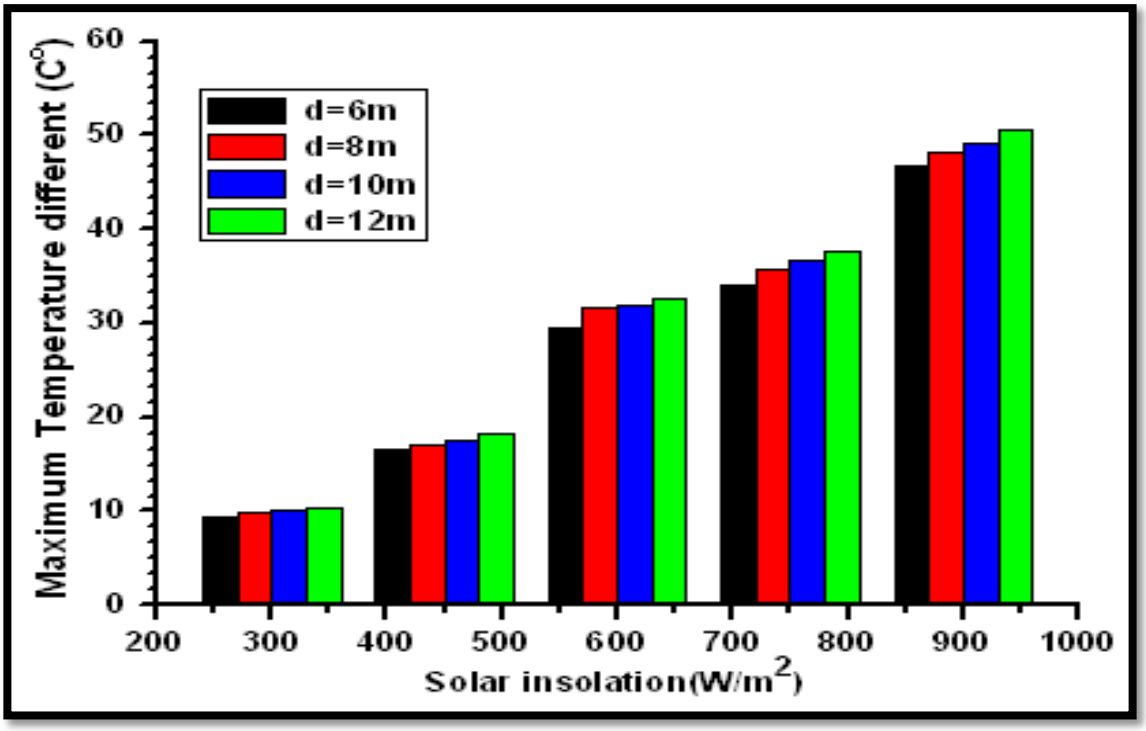

Figure 16. The effect of collector diameter on maximum temperature different at different solar insolation for H =6m.

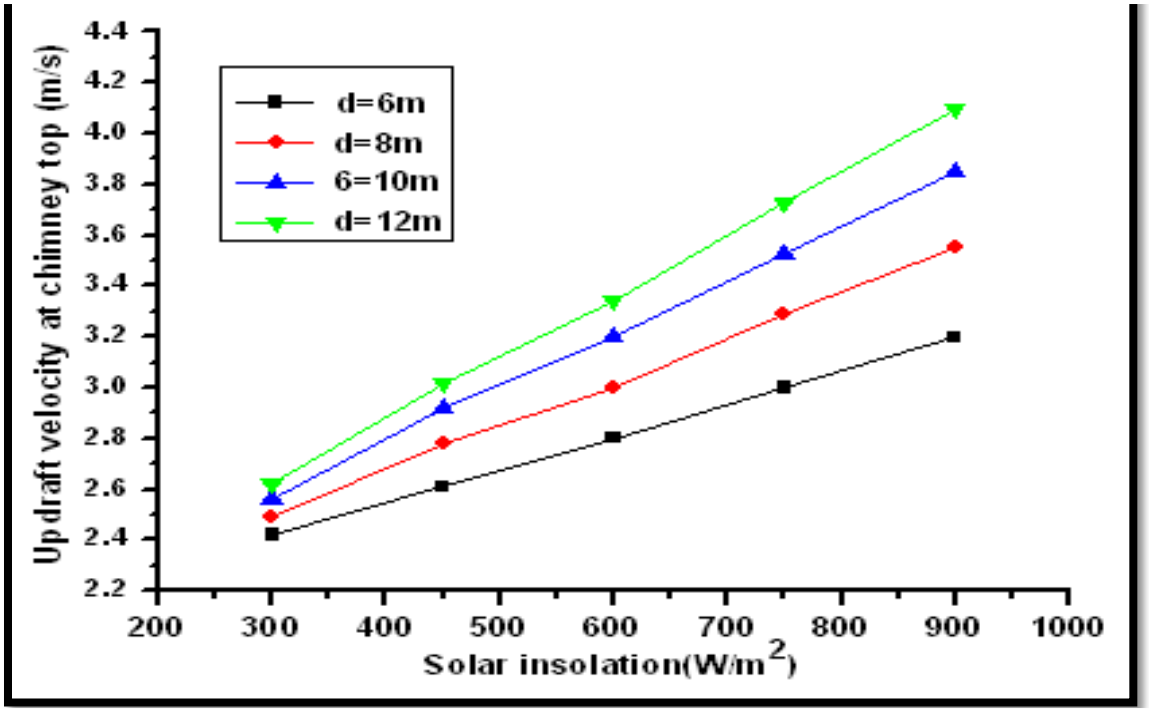

Figure 17. The effect of collector diameter on updraft velocity at chimney top at different solar insolation for H =6m.

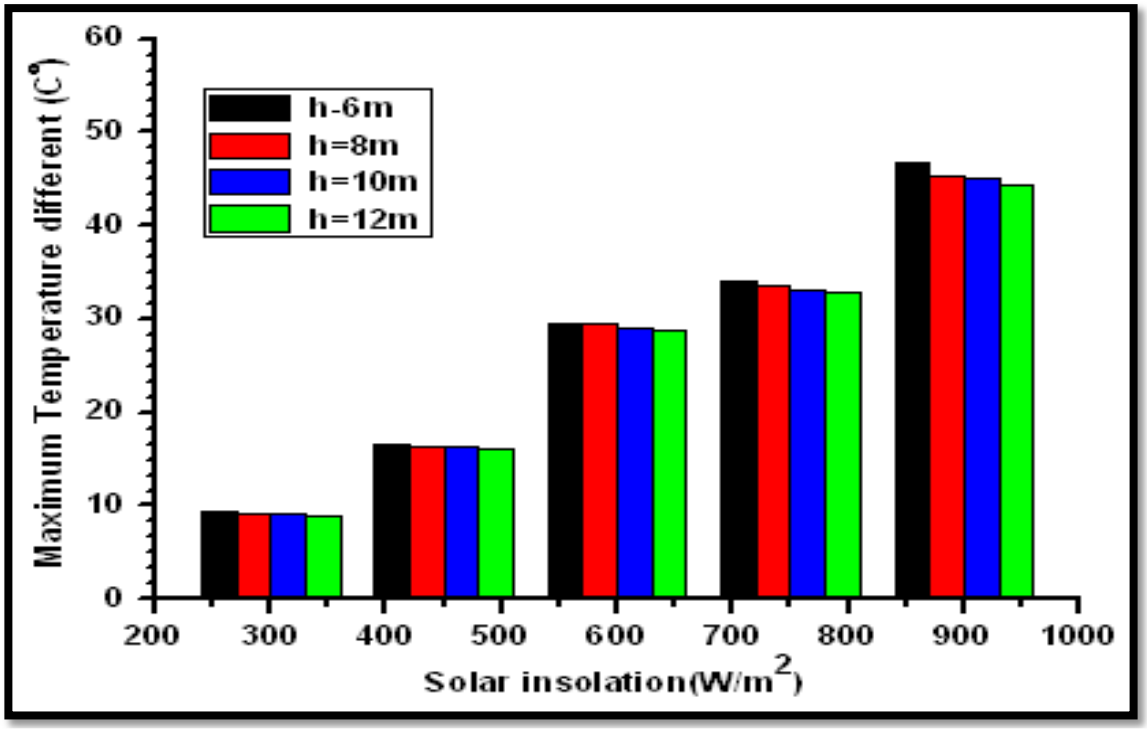

Figure 18. The effect of chimney height on maximum temperature different at different solar insolation for D =6m.

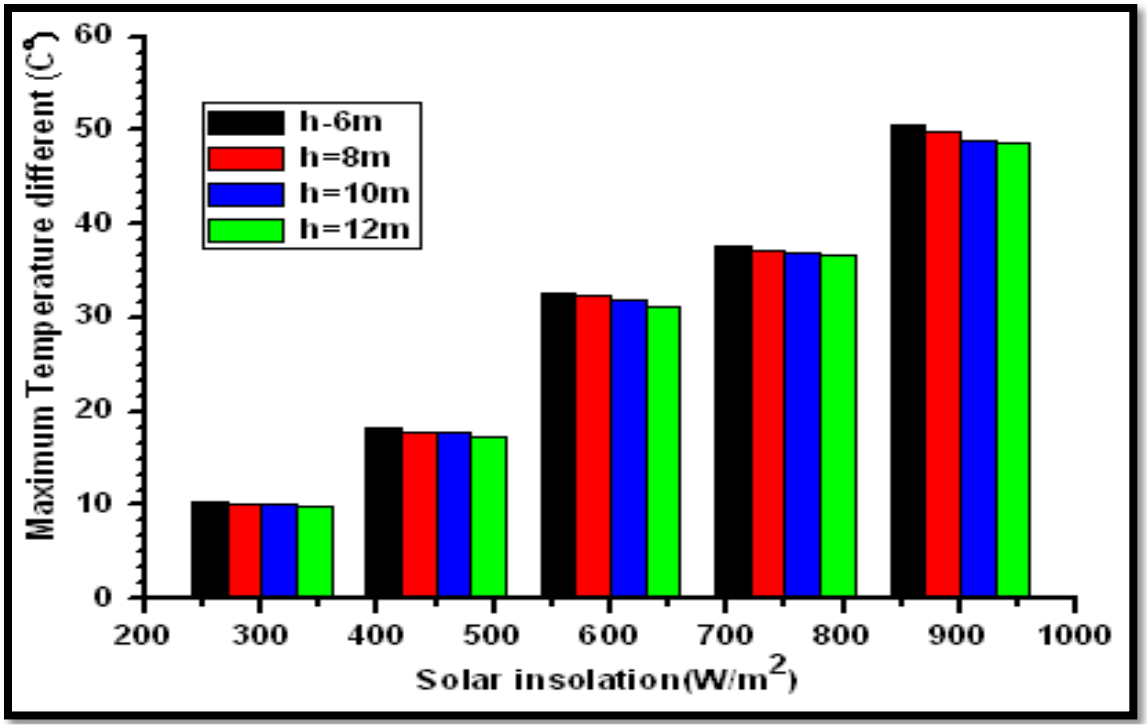

Figure 19. The effect of chimney height on maximum temperature different at different solar insolation for D =12m.

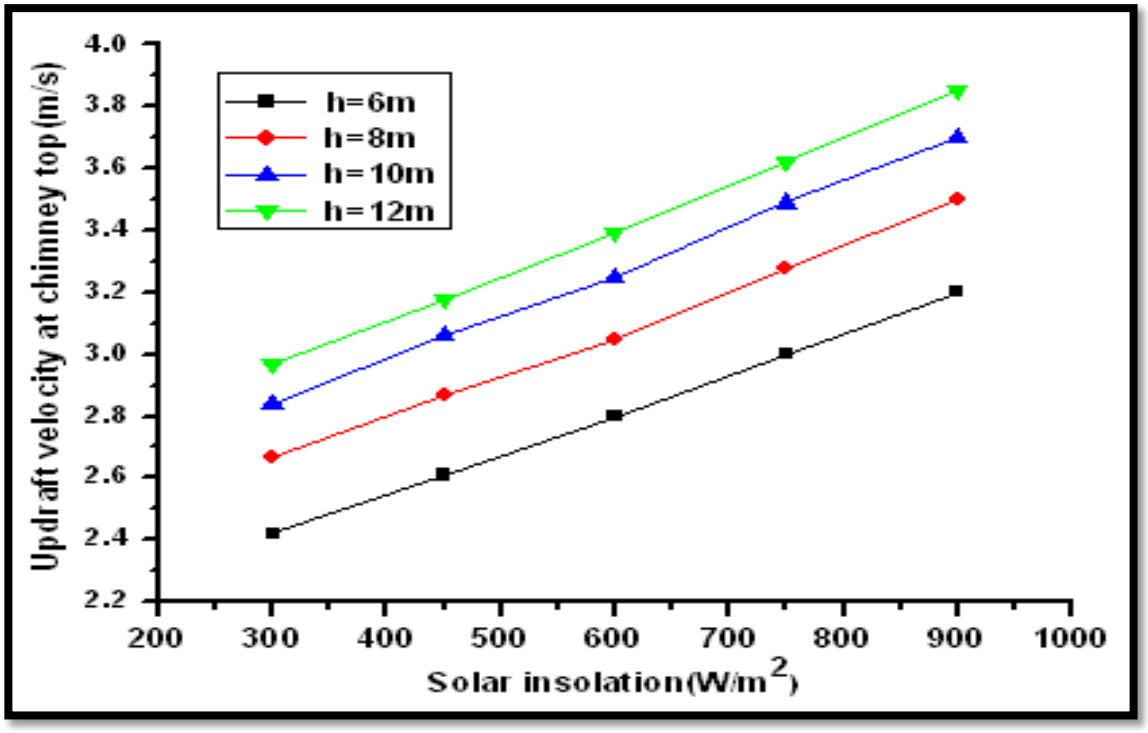

Figure 20. The effect of chimney height on updraft velocity at chimney top at different solar insolation for D =6m.

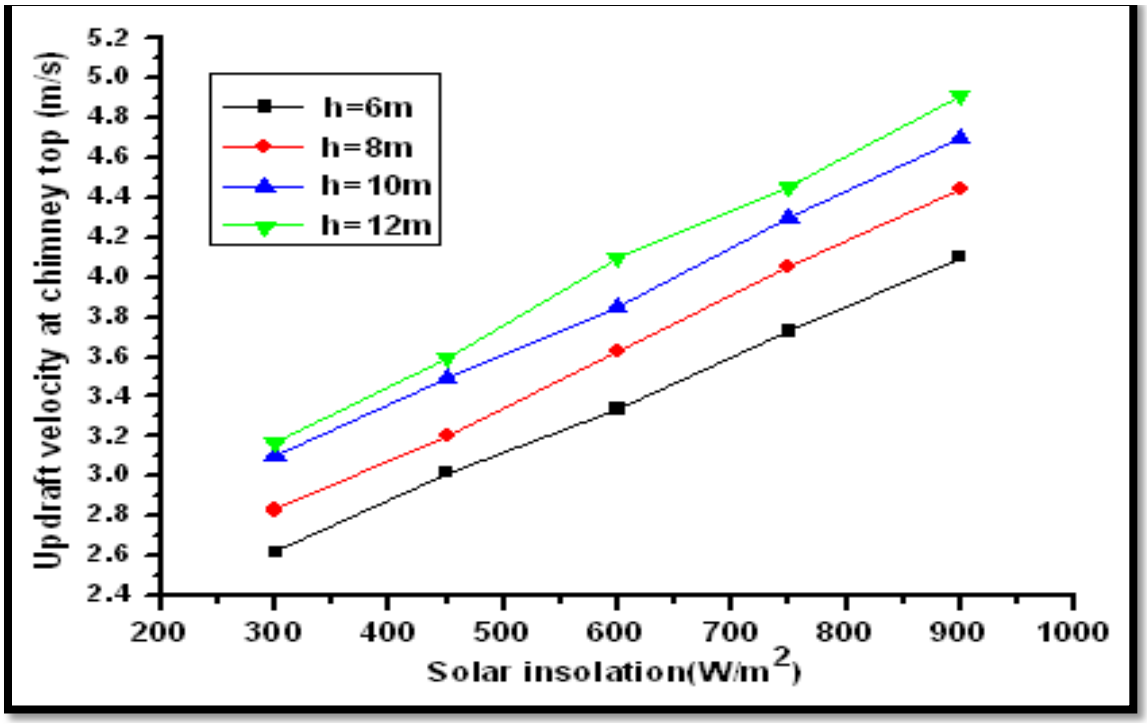

Figure 21. The effect of chimney height on updraft velocity at chimney top at different solar insolation for D =12m.

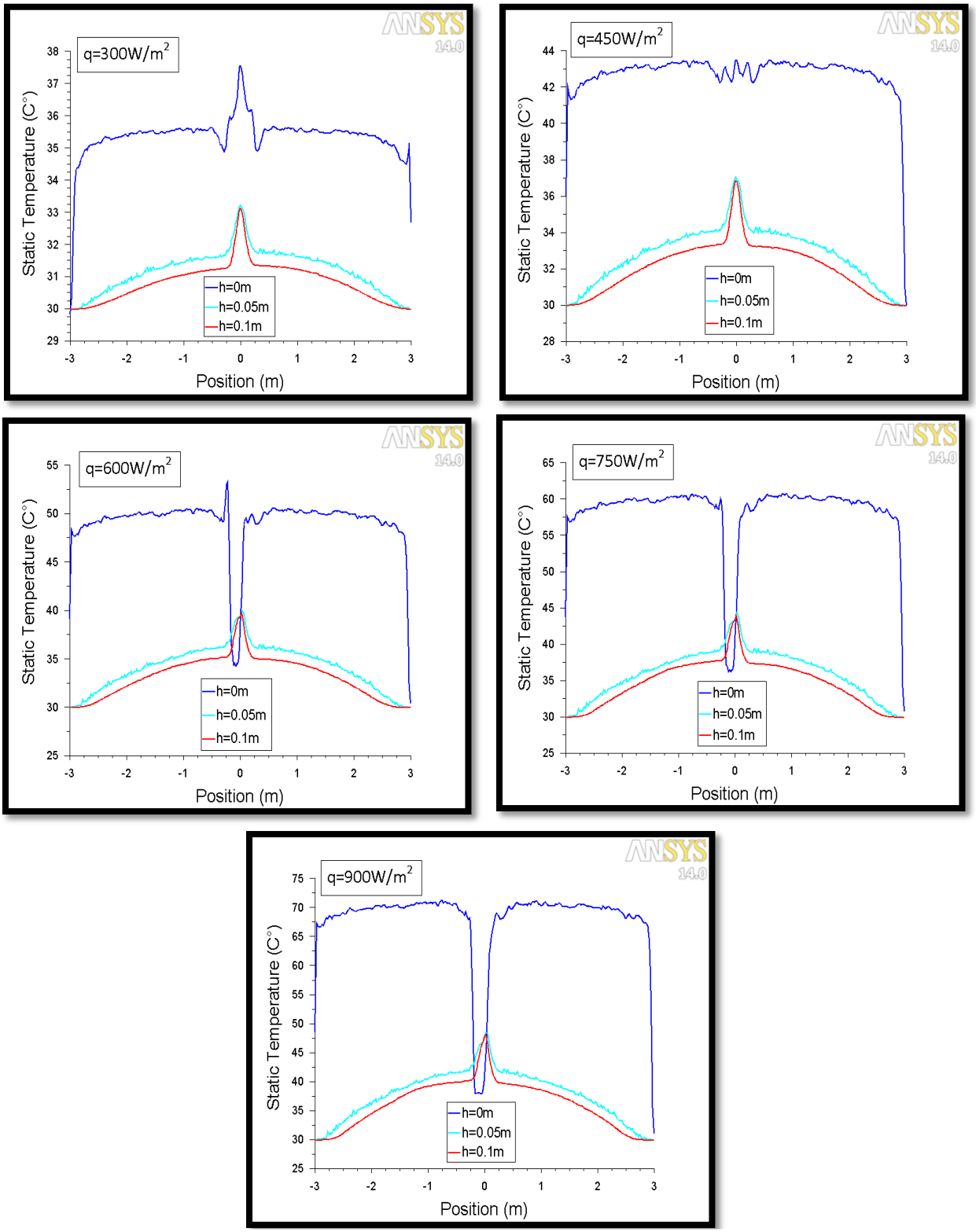

Figure 22. Air temperature at different heights above the ground level in the solar collector and at different solar insolation for D =6m, H =12m.

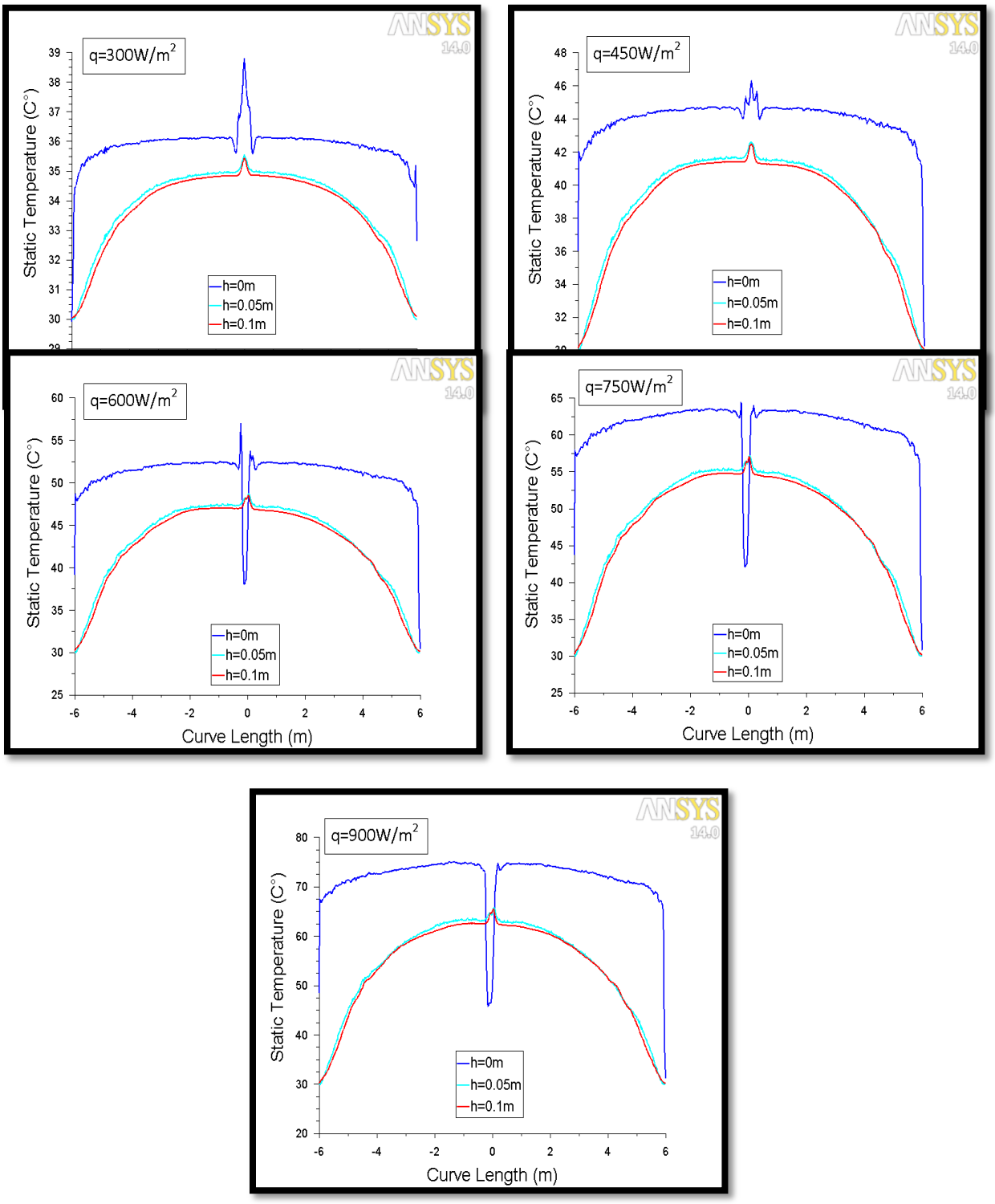

Figure 23. Air temperature at different heights above the ground level in the solar collector and at different solar insolation for D =12m, H =6m.